Supporting Information

Controllable Self-Assembly of Micro-Nanostructured Si-embedded Graphite/Graphene Composite Anode for High-Performance Li-ion Batteries

Ning Lin, Tianjun Xu, Tieqiang Li, Ying Han, Yitai Qian**

Department of chemistry, university of science and technology of china, Hefei Anhui province, 230026, P. R. china. Email: *ningl@mail.ustc.edu.cn*, *ytqian@ustc.edu.cn*

Experimental Section

Mechanical ball milling of Si and graphite： Micro-sized Si (99% purity, 200 mesh) was introduced into a zirconium dioxide vials with a ball-to-powder mass ratio of 15 :1, then ball-milled at room temperature for 24 h at a speed of 600 r min^{-1}. Similarly, the commercial graphite particles (d_{50}=15μm) were milled at a speed of 300 r/min for 5 h. The milled Si and graphite products were collected for further application.

Preparation of graphene oxide suspension: Graphite oxides (GO) powder was made according to a modified Hummer's method. As collected GO powder was dispersed in water and ultrasonicated for 1 h. After 4000 rpm centrifuge for 10 min, a brown homogeneous supernatant was obtained. Then, dispersed GO suspension with 1 mg mL^{-1} was obtained by diluted the GO solution with appropriate water.

Materials characterization: The structure and morphology of as-prepared products were characterized by X-Ray diffraction (XRD, Philips X'Pert Super diffractometer with Cu Kα radiation (λ=1.54178Å)), Raman spectrometer (Lab-RAM HR UV/VIS/NIR), scanning electron microscopy (SEM, JEOL-JSM-6700F), and transmission electron microscopy (TEM, JEOL; 2010); the thermo-gravimetric analysis (TGA Q5000IR system) under an air atmosphere; Nitrogen adsorption-dsorption analysis (ASAP 20202020 M+C, Micromeritics) at 77 K.

Electrochemical measurement: The Li-ion storage performance of the as-prepared materials were tested with half-cells (CR2016) which were carefully assembled in an argon-filled glove box (H_2O, O_2 < 0.1 ppm). The Li metal foil is served as the counter/reference electrode, the electrolyte is a solution of 1 M $LiPF_6$ in ethylene carbonate and diethyl carbonate (1:1 in volume ratio). The slurry mixture of the as-synthesized anode material, super P, and carboxymethylcellulose sodium (CMC-Na) with a weight ratio of 70: 15: 15 was coated on Cu foil (99.9%) and dried. Noted, we adopted a copper wafer with diameter size of 12 mm, the mass loading of active materials on each electrode was 2.0 mg approximately. Galvanostatic charge/discharge cycling performance were measured on a LAND-CT2001A instrument under a voltage range of 0.01−1.5 V (vs. Li/Li^+). Cyclic voltammetry (CV) and Electrochemical impedance spectroscopy (EIS) were performed on an electrochemical workstation (CHI660D) at room temperature. Noted, the current density 1C of graphite, Si, SGG anode and SG are set as 370, 3600, 600 and 700 mA g^{-1}, respectively.

The full-cell was assembled based on the as-prepared SGG anode and the commercially available $LiFePO_4$ cathode. The anode was prelithiated using Li metal in half-cell in order to form stable SEI film, and compensate the initial Li loss. The full cell was designed to anode limited, with cathode/anode capacity ratio of *ca.* 1.1/1. The current density and the specific capacity is calculated based on the weight of the SGG anode. The used electrolyte and the separator are same as that of in half-cell. The cutoff potential window of full cell during galvanostatic discharge/charge measurements is 2-3.8 V.

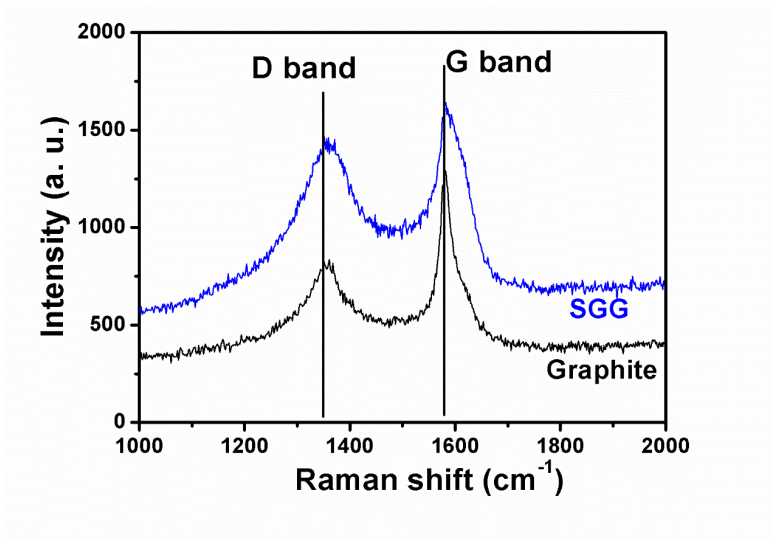

Figure S1. Raman spectra of SGG and graphite samples.

The Raman spectrum was measured to evaluate the disorder carbon contents in the composite. As shown in **Figure S1,** the Raman spectrum of graphite and SGG displays two strong peaks at 1350 and at 1580 cm^{-1}, corresponding to the D and G-bands, respectively. The G-band is attributed to the first order scattering of the E2g phonon of the sp2 carbon-carbon bond; while the D-band represents the defect sites associated

with vacancies and grain boundaries. Generally, the intensity ratio of I_D/I_G provides direct evidence of the degree of graphitization. The SGG composite shows higher I_D/I_G than that of commercial graphite (0.84 vs 0.62), indicating more defects in the SGG composite.

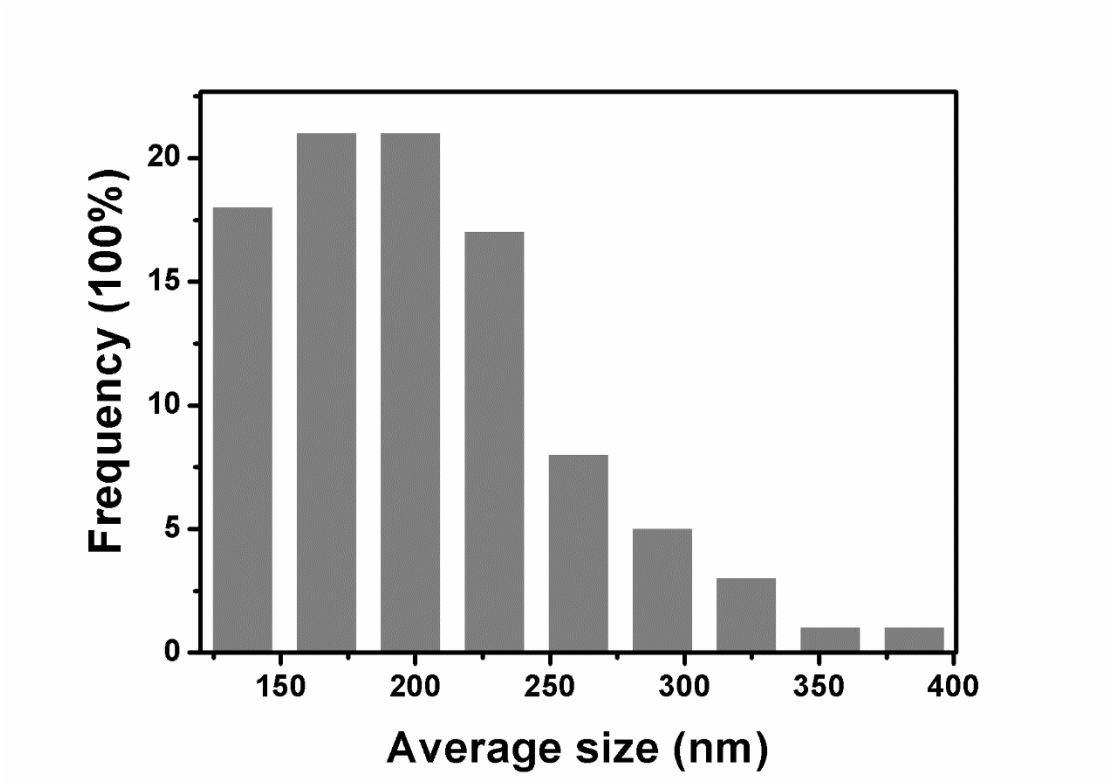

Figure S2 particles size distribution of Si.

The average size of Si particles is 190, ranging from 120 to 380 nm.

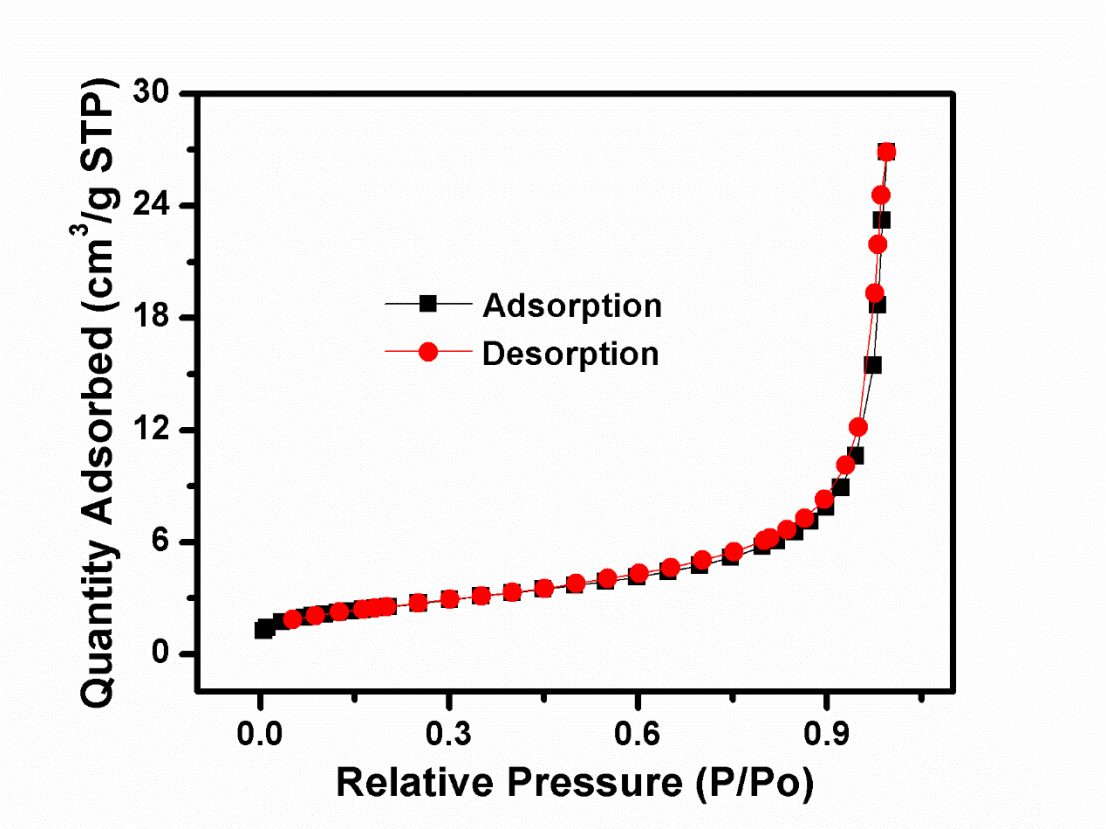

Figure S3. The Nitrogen adsorption-desorption isotherms of the SG composite.

Figure S3 shows the nitrogen adsorption and desorption isothermal of the SG sample. The calculated BET specific surface area of the SG are 13.0 m^2 g^{-1}, which is a bit higher than that of graphite, but lower than that of SGG composite.

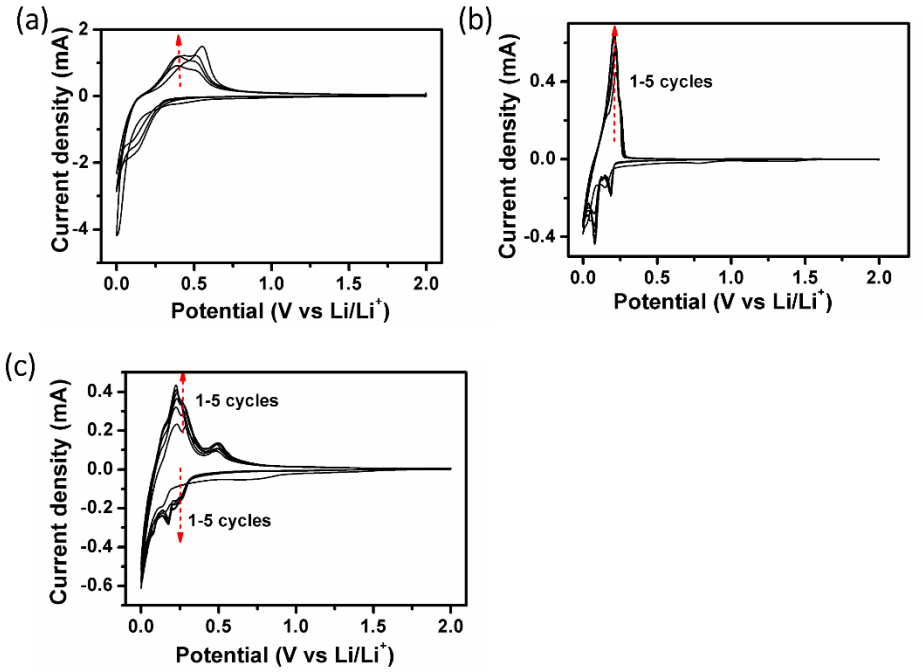

Figure S4 The CV curves of the (a) Si, (b) graphite, and (c) SGG based electrodes.

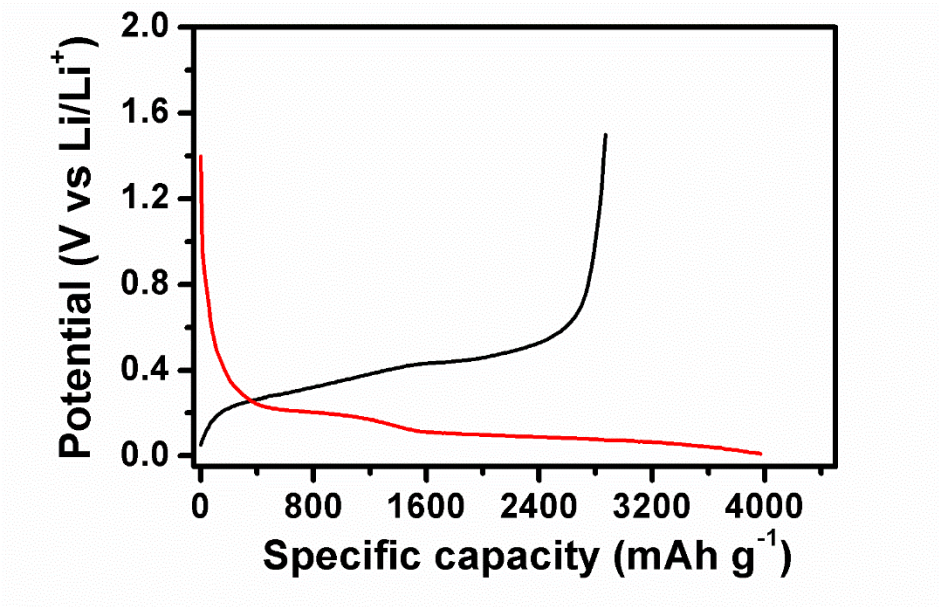

Figure S5 The discharge/charge capacity potential profile of the ball-milled Si electrode.

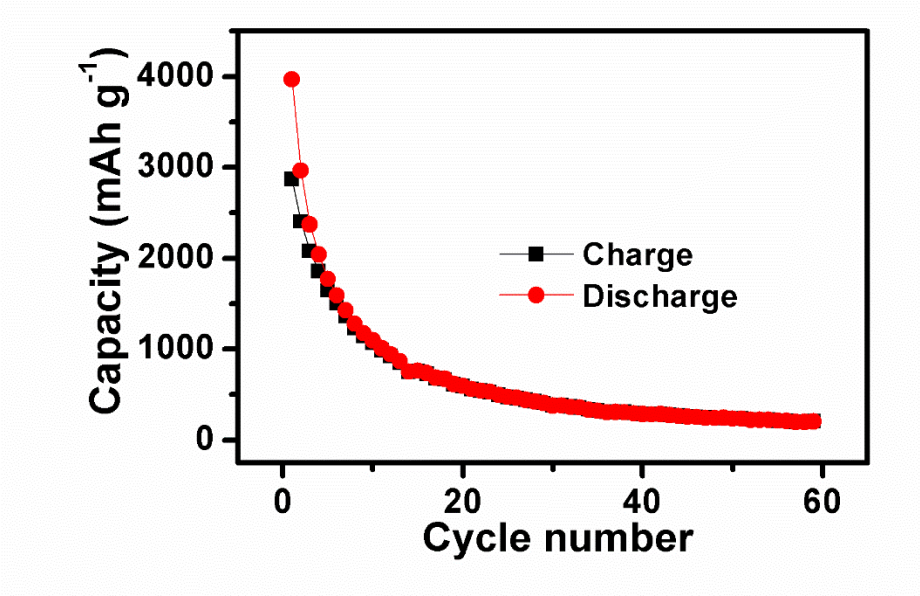

Figure S6 The cycling properties of the ball-milled Si electrode.

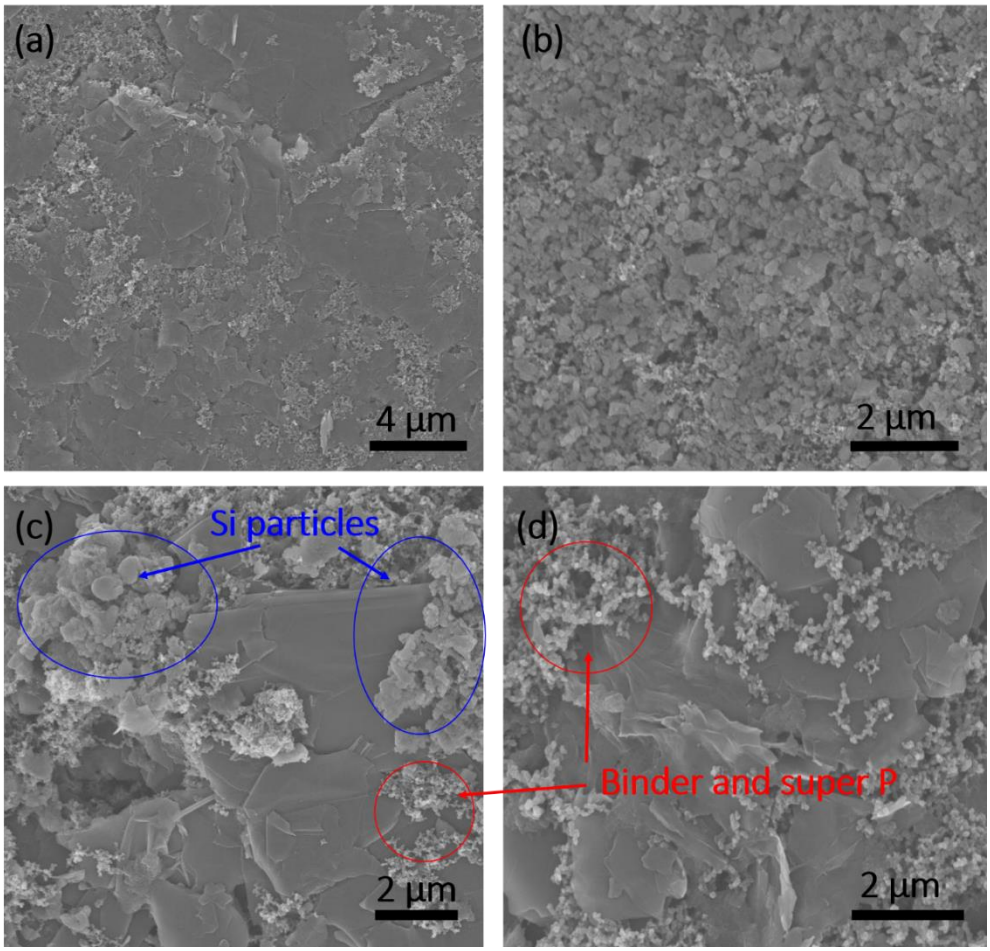

Figure S7 The SEM images of the fresh electrode surface of (a) graphite, (b) Si, (c) SG, and (d) SGG samples.

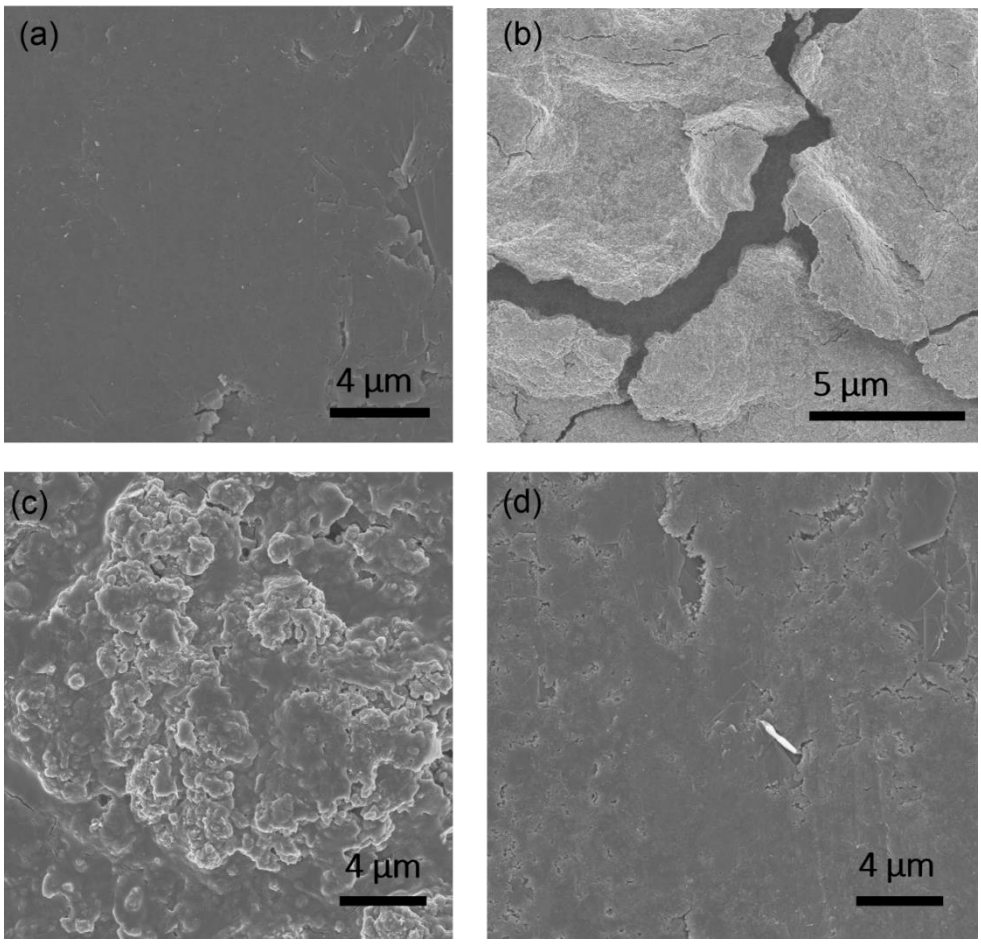

Figure S8 The SEM images of the electrode surface change after 100 cycles of (a) graphite, (b) Si, (c) SG, and (d) SGG samples.

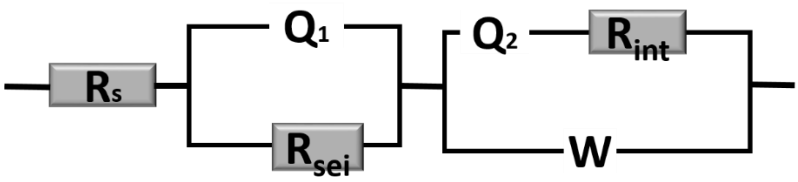

Figure S9 The corresponding equivalent circuit.

Rs (also known as the solution resistance) is the equivalent series resistance, which generally describes the resistance of the electrolyte combined with the internal

resistance of the electrode. The Rsei are corresponding to the SEI film resistance (first high-frequency semicircle). The Rint corresponds to the interphase electronic contact resistance in the electrode/electrolyte interface (second semicircle).

Table S1. Simulation results of the kinetic parameters of the Si, SG (si/graphite), G (graphite), and SGG based electrodes.

	R_s	R_{sei}	R_{int}
Si (before cycling)	2.83	0.10	119.9
Si (20 cycles)	3.25	73.01	197.3
SG (before cycling)	0.99	0.13	107.5
SG (20 cycles)	1.08	8.35	180.1
G (before cycling)	1.05	0.60	76.3
G (20 cycles)	0.87	8.81	99.1
SGG (before cycling)	0.89	0.01	62.2
SGG (20 cycles)	1.02	5.7	107.5

The corresponding resistance of different sample are calculated. Table S1 exhibits the simulation results of the kinetic parameters. As can be seen, the Rs of different electrodes maintain at low value constantly whether cycling or not. Before discharge/charge cycling, the SGG electrode shows the lowest Rint value (62.2 Ohm), while the Si electrode shows the highest (119.9 Ohm). After 20 cycles, the Rint resistance of Si are increased remarkably to 197.3 because the huge volume change destroy the conductive integrity of electrode, While, the Rint resistance of SGG based electrode shows less growth (107.5 Ohm) that is close to that of graphite electrode. On

the other hand, the Rsei resistance of Si electrode has increased significantly to 73.01 ohm which is far bigger than that of the other samples, because the repeat volume change would cause the formation of thicker SEI film. This result indicates that graphite and graphene is able to stabilize the SEI.

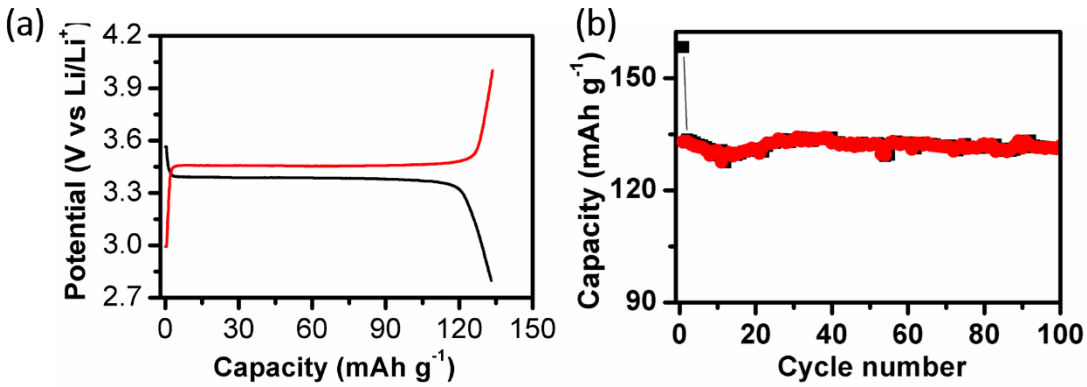

Figure S10 (a) Charge-discharge profile (b) Charge/discharge capacity at a current density of 1C the commercially available $LFePO_4$ cathode.